

H₂O Fluid Distribution in Mantle Rock at 1 GPa : Constraints from Vs-Vp/Vs Diagram

Hiroki Sato^{1)*} and Kazuhiko Ito²⁾

¹⁾ Department of Earth and Space Science, Osaka University

²⁾ Faculty of Business Administration, Southern Osaka University

Abstract

We investigate the distribution of H₂O fluid in the olivine-pyroxene-H₂O system produced by the dehydration of serpentinite, using P- and S-wave velocities measured simultaneously as a function of temperature at 1 GPa. Serpentine and brucite in serpentinite break down at high temperatures, and the rock sample consists of olivine, pyroxene, and H₂O at ~900°C and 1 GPa. A Vs-Vp/Vs diagram is adapted to analyze the dehydration process from seismic velocity data. Employing Grüneisen theory and third-order finite strain theory, we calculate elastic-wave velocities in a dry olivine-pyroxene solid. Then P- and S-velocities are estimated for various H₂O fluid distributions (tubes, disks, and films) in the olivine-pyroxene-H₂O system. At temperatures above complete dehydration of serpentinite, laboratory velocity data are reproduced using numerical calculations for triangular tubes of H₂O fluid distribution. The results indicate that after dehydration is completed, elastic properties of serpentinite are estimated from those calculated for the olivine-pyroxene-H₂O system.

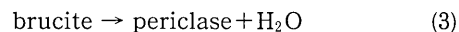
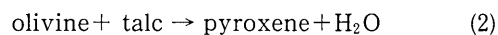
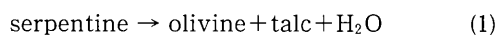
Key words: serpentinite, olivine-pyroxene-H₂O system, Vs-Vp/Vs diagram, fluid distribution, dehydration process

1. Introduction

A sharp velocity decrease is commonly observed with dehydration of rocks containing hydrous minerals (e.g., Kern and Fakhimi, 1975; Ito, 1990; Lebedev *et al.*, 1991; Popp and Kern, 1993). P-wave velocities in serpentinite including 75% antigorite were measured up to 700°C at 0.2 GPa by Kern and Fakhimi (1975). They observed a rapid velocity drop due to the breakdown of antigorite. Similar P-velocity drops were reported for serpentinite by Lebedev *et al.* (1991) and for basalt and graywacke by Kern (1990). Popp and Kern (1993) measured both P- and S-wave velocities (Vp and Vs, respectively) in serpentinite to 750°C at 0.2 GPa. Rapid decreases of Vp, Vs, and Poisson's ratio were observed above 650°C, indicating the onset of dehydration. Their results were interpreted in terms of crack density and fluid saturation using the self-consistent approximation of O'Connell and Budiansky (1974). For serpentinite,

Popp and Kern (1993) obtained increases of crack density to 0.15-0.2 and decreases of fluid saturation to ~0.4 as temperature increased. In the studies by Kern and Fakhimi (1975), Lebedev *et al.* (1991) and Popp and Kern (1993), the rock samples were not sealed, and measurements were carried out in open systems.

For the first time, Ito (1990) determined both P- and S-wave velocities in serpentinite, which was entirely sealed in a nickel capsule, as a function of temperature to ~900°C at 1 GPa using a piston-cylinder high-pressure apparatus (Fig. 1). The serpentinite was collected at Ehime, Japan, and consisted of serpentine, olivine, and brucite. The following dehydration reactions successively occurred in the rock sample.



*e-mail : roki@ess.sci.osaka-u.ac.jp (1-1, Matikane-yama-cho, Toyonaka, Osaka 560-0043 Japan)

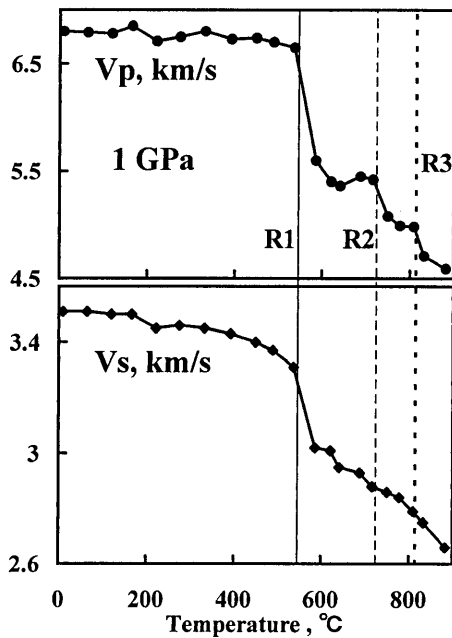


Fig. 1. P- and S-wave velocities in serpentinite measured as a function of temperature at 1 GPa by Ito (1990). R1, R2, and R3 correspond to the temperatures of the dehydration reactions (1), (2), and (3), respectively. Note rapid velocity decreases at dehydration temperatures.

Reactions (1) to (3) have been investigated in detail, and occur at about 550°C, 730°C, and 820°C, respectively, at 1 GPa (e.g., Kitahara *et al.*, 1966; Yamaoka *et al.*, 1970). A large amount of H_2O released from reaction (1) causes sharp velocity drops at 550°C for both P- and S-waves (Fig. 1). At a higher temperature, however, P-velocities appear to be affected more by reactions (2) and (3) than S-velocities. Later, similar P-velocity behavior was observed in serpentinite by Popp and Kern (1993).

To determine elastic-wave velocity in serpentinite, Ito (1990) used a pulse transmission technique with tourmaline transducers directly attached to the sample capsule. This allowed accurate travel-time measurements at high pressures and temperatures. Importantly, the tourmaline was cut in the crystallographic direction to generate both compressional and shear waves simultaneously. Both V_p and V_s were, thus, measured simultaneously at each temperature for the same rock sample. The sample was placed into a nickel capsule, which was sealed with silver solder. During the velocity measurements, therefore, reactions (1) to (3) occurred in a closed system. More details of the experimental procedures are described in Ito (1990).

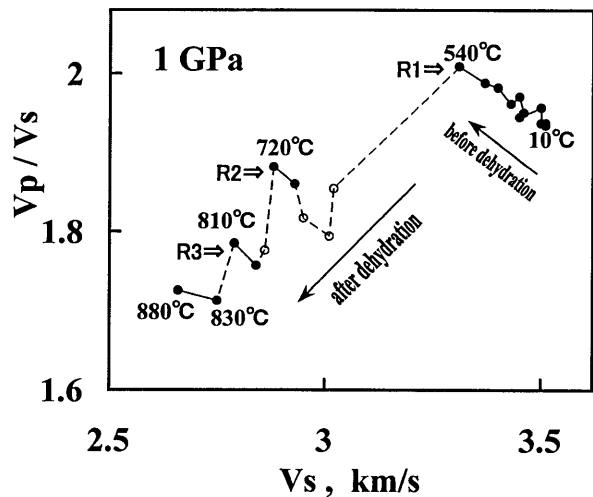


Fig. 2. V_s - V_p/V_s diagram in serpentinite at 1 GPa. R1, R2, and R3 are described in Fig. 1. Small travel-time increases persist and the sample is not equilibrated in the data shown by open circles with dashed lines. However, velocity changes with time are not observed in the data of closed circles with solid lines, and the sample is equilibrated in a short time. Note dramatic changes in the data trend after reactions (1) to (3). Before dehydration, V_p/V_s increases with increasing temperature; however, it rapidly decreases as dehydration proceeds.

Soon after the velocity measurement at 880°C and 1 GPa, the sample was quenched to room temperature and was examined using an electron microscope and X-ray analysis. Ito (1990) found that the dehydration reactions (1) to (3) had been completed, and major components of the sample were olivine, pyroxene (orthopyroxene), and H_2O . Periclase produced by reaction (3) was not observed, but was combined with pyroxene to form olivine. Therefore, the dehydration of serpentinite at $\sim 900^\circ\text{C}$ and 1 GPa yields the system of olivine-pyroxene- H_2O .

2. Methods and Results of Analysis

We calculated velocity ratios V_p/V_s from the data by Ito (1990) (Fig. 1), and find a good correlation between V_p/V_s and V_s (Fig. 2), rather than V_p/V_s and V_p . Here we use a V_s - V_p/V_s diagram to investigate the dehydration process of serpentinite. Before dehydration, V_p/V_s increases and V_s decreases with increasing temperature, therefore, the data tend upwards to the left in Fig. 2. After dehydration, however, V_p/V_s decreases with temperature as dehydration reactions proceed, and the data tend downwards to the left. Small travel-time increases persist in the velocity data taken directly after reactions (1) and (2)

(open circles in Fig. 2). However, velocity changes with time are not observed in the data taken directly before reactions (2) and (3), and the data at 830°C and 880°C (closed circles in Fig. 2). This indicates that the rock sample is equilibrated in a short time (less than 10 minutes). In the Vs-Vp/Vs diagram, equilibrated data show an increase of Vp/Vs with an increase of temperature, although mineral dehydration reactions, in general, cause a decrease of Vp/Vs. Shear modulus and so Vs are much more sensitive to temperature than bulk modulus in mantle rocks (e.g., Sumino and Anderson, 1984; Anderson, 1989), therefore, temperature increase reduces Vs and increases Vp/Vs, as observed in the closed symbols in Fig. 2. Dramatic changes in both Vs and Vp/Vs, particularly after reaction (1), are due not only to the occurrence of H₂O fluid, but also to changes in the solid component from serpentine to olivine and talc. A Vs-Vp/Vs diagram is a powerful tool to study and analyze rock dehydration processes from seismic velocity data.

One can numerically calculate elastic-wave velocities in olivine and pyroxene at high pressures and temperatures, following the method described by Duffy and Anderson (1989) and Sato *et al.* (1998). The effects of fluid on seismic velocity were numerically estimated by Mavko (1980) and Schmeling (1985). Therefore, P- and S-wave velocities in an olivine-pyroxene-H₂O system are calculated using available elasticity data for H₂O fluid. We first calculated velocities in a dry solid phase (olivine-pyroxene) at 1 GPa and a high temperature, from mineral elasticity data. We then incorporated the effects of H₂O on velocity, following the method described by Schmeling (1985), and obtained Vp and Vs in the olivine-pyroxene-H₂O system.

2.1. Calculation of Velocity in Dry Olivine-Pyroxene System

After dehydration is completed, the serpentinite sample at 880°C and 1 GPa consists of olivine 83.4%, pyroxene 7.0%, and H₂O 9.6% by weight (Ito, 1990). For olivine and pyroxene (for elastically isotropic mineral aggregate), elastic-wave velocities at high pressures and temperatures are estimated from laboratory elasticity data for an isotropic mineral aggregate. First, we calculated densities, elastic constants, and pressure derivatives at a given temperature at one atmosphere, using the method described by

Duffy and Anderson (1989). We considered the effects of anharmonicity on seismic velocity. The one-atmosphere physical properties calculated at a high temperature were then extrapolated adiabatically for high pressures. Third-order finite strain theory yields P- and S-wave velocities, Vp and Vs, respectively, at high pressure P as (e.g., Davies, 1974; Duffy and Anderson, 1989)

$$\begin{aligned}\rho V_p^2 &= (1-2\varepsilon)^{5/2} L [1 + (5-3KL'/L)\varepsilon] \\ \rho V_s^2 &= (1-2\varepsilon)^{5/2} G [1 + (5-3KG'/G)\varepsilon] \\ P &= -3\varepsilon(1-2\varepsilon)^{5/2} K [1 + (6-3K'/2)\varepsilon]\end{aligned}\quad (4)$$

with $\varepsilon = [1 - (\rho/\rho_a)^{2/3}]/2$ and $L = K + 4G/3$,

where ρ is the density, ρ_a is the density at one atmosphere, ε is the strain, K is the adiabatic bulk modulus, and G is the shear modulus. Primes refer to pressure derivatives. Temperature, T, was calculated as a function of pressure using equation

$$T(P) = T_a + \int_0^P (\gamma T/K) dP \quad (5)$$

where T_a is a given temperature and γ is the Grüneisen parameter. Empirically, the Grüneisen parameter is found to decrease with pressure as $\gamma = \gamma_a (\rho/\rho_a)^{-q}$ ($q \cong 1$) (Jeanloz and Knittle, 1986). However, the density increase is no more than 3%, when pressures increase from 0 to 3 GPa. Thus, the pressure dependence of the Grüneisen parameter does not cause errors (much less than 0.5%) in calculations of adiabatic temperature from equation (5). Here we employ $\gamma = 1.1$ regardless of pressure (e.g., Isaak, 1992).

Using equations (4) and (5) and elasticity data given by Duffy and Anderson (1989), P- and S-wave velocities in olivine and pyroxene were computed as a function of pressure and temperature. The velocities V_{po} and V_{so} in the olivine-pyroxene solid of the run product at 1 GPa and high temperatures were then calculated taking a Voigt-Reuss-Hill (VRH) average (Hill, 1952). The calculated V_{po}, V_{so}, and density ρ_o are listed in Table 1. Following the method described here, we were able to compute Vp, Vs, and ρ of peridotite with variable olivine and pyroxene contents at pressures to ~ 3 GPa and temperatures approaching the solidus temperature.

2.2. Calculation of Velocity in Olivine-Pyroxene-H₂O System

The presence of liquid phase reduces seismic velocity to a degree that depends on the amount and geometry of a fluid. At fractions below several percent, fluids in isolated pores (disks) cause only weak

reductions of velocity, but fluid films (sheets) produce sharp velocity drops. Liquid-filled tubes provide effects much less than films, but stronger than disks. The seismic behavior of a solid containing randomly-oriented cracks with partial saturation of fluid was described by O'Connell and Budiansky (1974). Later, Mavko (1980) and, in complete form, Schmeling (1985) derived theoretical expressions for elastic-wave velocity of fluid tubes.

To calculate P- and S-wave velocities in a H₂O-bearing rock, we follow the method described by Schmeling (1985). Velocities in a solid-H₂O system depend on the geometry of the intercrystalline fluid phase. Schmeling (1985) corrected incompleteness of Mavko's formulation, and described the elasticity of fluid inclusions covering a broad range of geometries including tubes, disks, and films. We calculated V_p

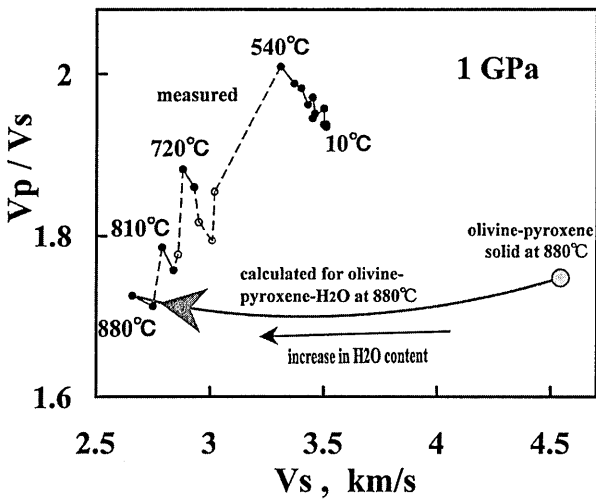


Fig. 3. Vs-Vp/Vs diagram in serpentinite (measured, same as Fig. 2) and olivine-pyroxene-H₂O system (arrow, $\kappa=2.0$) at 1 GPa. A large circle is V_{so}-V_{po}/V_{so} in a dry olivine-pyroxene solid at 1 GPa and 880°C (see Table 1). Along the arrow, H₂O content increases from 0 to 9.6 wt.%. The laboratory data are consistent with numerical calculations for tube geometry of H₂O fluid distribution.

and V_s, and obtained V_p/V_s as a function of H₂O content for various geometries. The compressional velocity, V_{pw}, and the density, ρ_w , of H₂O at 1 GPa and high temperatures used in this calculation are listed in Table 1. We employed elasticity data for pure H₂O, because only small amounts of silicates dissolve in H₂O at 1 GPa (e.g., Zhang and Frantz, 2000). The results of the calculation at 880°C are shown in Vs-V_p/V_s diagram in Fig. 3, with the laboratory data of Ito (1990). Only the tube geometry fits the laboratory velocity data, and the best fit at 1 GPa and 880°C with 9.6 wt.% H₂O gives a tube-shape parameter, κ , of 2.0 (Table 1, Fig. 4). The cross-section of the tube is triangular for small κ (less than ~ 2), but is circular for $\kappa > \sim 2$ (Fig. 4; Mavko, 1980). The data measured at 830°C by Ito (1990) also fit the tube model with $\kappa=2.2$. On the other hand, V_p/V_s values are well below 1.7 for all parameter values in the disk geometry, that do not fit the laboratory data. Fur-

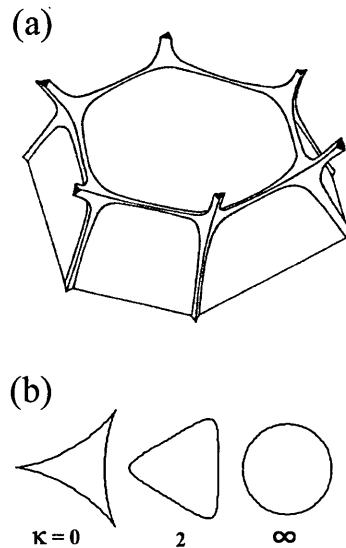


Fig. 4. Fluid tubes along grain edges (a), and the cross-section of tube with tube-shape parameter κ (b) (after Mavko, 1980).

Table 1. Physical parameters in olivine-pyroxene-H₂O system at 1 GPa

temperature °C	component of the run product			H ₂ O property *		olivine-pyroxene property			
	H ₂ O wt. %	olivine wt. %	pyroxene wt. %	V _{pw} km/s	ρ_w g/cc	V _{po} km/s	V _{so} km/s	ρ_o g/cc	κ
830	9.6	83.4	7.0	1.99	0.893	7.97	4.57	3.28	2.2
880	9.6	83.4	7.0	1.96	0.874	7.94	4.54	3.28	2.0

* H₂O properties from Bowers (1995)

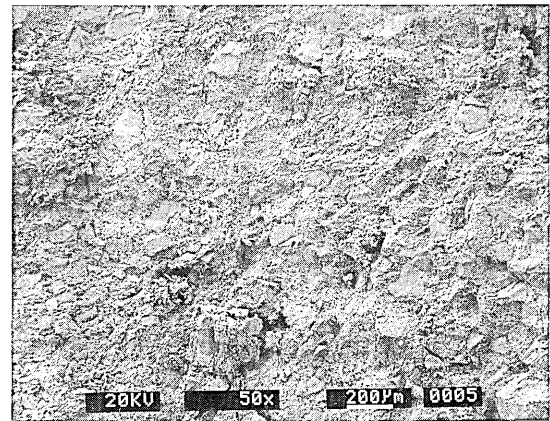
ther, the film geometry requests a rapid Vp/Vs increase even for a small H₂O content (e.g., 1 wt.%), and yields Vs=0 well below 9.6 wt.% H₂O. This is inconsistent with Ito's data.

3. Discussion

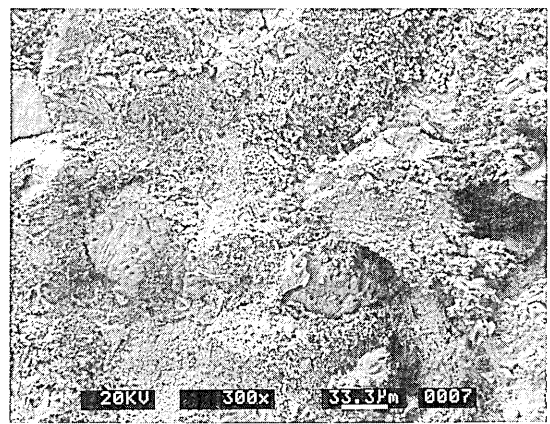
Fig. 5 shows images of the run product quenched after the velocity measurement at 880°C and 1 GPa. Pores that were filled with H₂O are observed at grain corners. The H₂O content of the rock sample (9.6 wt.%) is large enough to allow tube-like fluid interconnection (cf. von Bargen and Waff, 1986). In general, however, film-like spaces or voids were not found under the electron microscope. These observations support the results of the present analysis on the Vs-Vp/Vs diagram.

Equilibrium H₂O distributions in mantle rocks have been investigated in detail (e.g., Watson and Brenan, 1987; Watson and Lupulescu, 1993; Mibe *et al.*, 1998). Watson and Brenan (1987) investigated the equilibrium distribution of H₂O-CO₂ fluids in dunite (synthetic olivine aggregate) at 950–1150°C and 1 GPa. Their results show that the dihedral wetting angle, θ , varies from 65° for H₂O to 90° for 10% H₂O–90% CO₂, and is insensitive to the amount of salts added to pure H₂O. In pyroxenes, θ is also higher than 60° (Watson and Brenan, 1987; Watson and Lupulescu, 1993), indicating the existence of isolated pores at grain corners in upper mantle assemblages, if the H₂O content is less than ~2% (Bulau *et al.*, 1979; von Bargen and Waff, 1986). Watson *et al.* (1990) and Mibe *et al.* (1998) reported a decrease of the dihedral angle with an increase of temperature and pressure to 1200°C and 5 GPa, respectively. However, up to 900°C at 1 GPa, previous studies on equilibrium H₂O distribution in mantle rocks show $\theta > 60^\circ$. Therefore, H₂O exists in isolated pores for up to ~2% fluid. Above ~2%, on the other hand, fluids are no longer isolated but form interconnected networks, as pointed out by von Bargen and Waff (1986). In this study, the H₂O content (9.6 wt.%) is large enough to allow interconnection of pores and to form a tube geometry.

Studies on the hydrous mineral stability and the thermal structure of the subduction zone indicate the presence of volatiles and also serpentinites in the fore-arc mantle wedge (e.g., Niida and Green, 1999). These wet regions may be resolved by seismic tomo-



(a)



(b)

Fig. 5. Back scattered electron images of the run product quenched after the velocity measurement at 1 GPa and 880°C. Scale bars are 200 μm (a) and 33.3 μm (b). Pores that were filled by H₂O are observed. Most of the grains are olivines.

graphic studies. In fact, laboratory measurements generally show (e.g., Ito, 1990; Popp and Kern, 1993) that serpentinites have lower Vp and Vs and higher Vp/Vs than anhydrous mantle rocks, and that dehydration reduces Vp/Vs of seismic velocity. Monitoring both Vp and Vs structures of the mantle wedge is essential for understanding dehydration and hydration processes in the subduction zone.

4. Summary

We investigated the geometry of H₂O fluid distribution formed by the dehydration of serpentinite at 1 GPa using a Vs-Vp/Vs diagram. Above ~820°C, dehydration reactions in serpentinite are completed, and the rock sample consists of olivine, pyroxene, and H₂O. We calculated Vp and Vs in the olivine-pyroxene-H₂O system at 830°C and 880°C. Our calcu-

lations successively reproduce the velocities measured in the laboratory, by employing the tube geometry of the H₂O fluid distribution. This geometry is consistent with reported equilibrium H₂O distributions in mantle rocks, and is also supported by microscopic observations for the run product.

Acknowledgments

This work was supported by grants from JSPS (C12640467), and from Earthquake Research Institute, University of Tokyo (2001-A-18, Supervisor Dr. Y. Iio). We acknowledge Dr. S. Uehara for taking photomicrographs of the sample, and Dr. S. Yoshida and Dr. K. Mibe for helpful suggestions and comments.

References

- Anderson, D.L., 1989, *Theory of the Earth*, Blackwell Scientific Publications, Boston, 366 pp.
- Bowers, T.S., 1995, Pressure-volume-temperature properties of H₂O-CO₂ fluids, in "Rock Physics & Phase Relations: A Handbook of Physical Constants" edited by T.J. Ahrens, Am. Geophys. Union, Washington, DC, pp. 45-72.
- Bulau, J.R., H.S. Waff and J.A. Tyburczy, 1979, Mechanical and thermodynamic constraints on fluid distribution in partial melts, *J. Geophys. Res.*, **84**, 6102-6108.
- Davies, G.F., 1974, Effective elastic moduli under hydrostatic stress—I. quasi-harmonic theory, *J. Phys. Chem. Solids*, **35**, 1513-1520.
- Duffy, T.S. and D.L. Anderson, 1989, Seismic velocities in mantle minerals and the mineralogy of the upper mantle, *J. Geophys. Res.*, **94**, 1895-1912.
- Hill, R., 1952, The elastic behavior of a crystalline aggregate, *Proc. Phys. Soc. London*, **A65**, 349-354.
- Isaak, D. G., 1992, High-temperature elasticity of iron-bearing olivines, *J. Geophys. Res.*, **97**, 1871-1885.
- Ito, K., 1990, Effects of H₂O on elastic wave velocities in ultrabasic rocks at 900°C under 1 GPa, *Phys. Earth Planet. Inter.*, **61**, 260-268.
- Jeanloz, R. and E. Knittle, 1986, Reduction of mantle and core properties to a standard state by adiabatic decompression, in "Chemistry and Physics of the Terrestrial Planets", edited by S. K. Saxena, Springer-Verlag, New York, pp. 275-309.
- Kern, H., 1990, Laboratory seismic measurements: an aid in the interpretation of seismic field data, *Terra Nova*, **2**, 617-628.
- Kern, H. and M. Fakhimi, 1975, Effect of fabric anisotropy on compressional-wave propagation in various metamorphic rocks for the range 20-700°C at 2 kbars, *Tectonophysics*, **28**, 227-244.
- Kitahara, S., S. Takenouchi and G. C. Kennedy, 1966, Phase relations in the system MgO-SiO₂-H₂O at high temperatures and pressures, *Am. J. Sci.*, **264**, 223-233.
- Lebedev, E.B., A.M. Dorfman and S.R. Zebrin, 1991, Study of the mechanism of the influence of water on elastic wave propagation in amphibolites and some metamorphic rocks at high pressures and temperatures, *Phys. Earth Planet. Inter.*, **66**, 313-319.
- Mavko, G.M., 1980, Velocity and attenuation in partially molten rocks, *J. Geophys. Res.*, **85**, 5173-5189.
- Mibe, K., T. Fujii and A. Yasuda, 1998, Connectivity of aqueous fluid in the Earth's upper mantle, *Geophys. Res. Lett.*, **25**, 1233-1236.
- Niida, K. and D. H. Green, 1999, Stability and chemical composition of pargasitic amphibole in MORB pyrolyte under upper mantle conditions, *Contrib. Mineral. Petrol.*, **135**, 18-40.
- O'Connell, R.J. and B. Budiansky, 1974, Seismic velocities in dry and saturated cracked solids, *J. Geophys. Res.*, **79**, 5412-5426.
- Popp, T. and H. Kern, 1993, Thermal dehydration reactions characterized by combined measurements of electrical conductivity and elastic wave velocities, *Earth Planet. Sci. Lett.*, **120**, 43-57.
- Sato, H., K. Muro and A. Hasegawa, 1998, Three-dimensional mapping of magma source and transport regions from seismic data: the mantle wedge beneath northeastern Japan, *Pure Appl. Geophys.*, **153**, 377-398.
- Schmeling, H., 1985, Numerical models on the influence of partial melt on elastic, anelastic and electric properties of rocks. Part I: elasticity and anelasticity, *Phys. Earth Planet. Inter.*, **41**, 34-57.
- Sumino, Y. and O.L. Anderson, 1984, Elastic constants of minerals, in "CRC Handbook of Physical Properties of Rocks, Vol. III", edited by R. S. Carmichael, CRC Press, Boca Raton, Florida, pp. 39-138.
- Von Bargen, N. and H.S. Waff, 1986, Permeabilities, interfacial areas and curvatures of partially-molten systems: results of numerical computations of equilibrium microstructures, *J. Geophys. Res.*, **91**, 9261-9276.
- Watson, E.B. and J.M. Brenan, 1987, Fluids in the lithosphere, 1. experimentally-determined wetting characteristics of CO₂-H₂O fluids and their implications for fluid transport, host-rock physical properties, and fluid inclusion formation, *Earth Planet. Sci. Lett.*, **85**, 497-515.
- Watson, E.B., J.M. Brenan and D.R. Baker, 1990, Distribution of fluids in the continental mantle, in "Continental Mantle", edited by M.A. Menzies, Clarendon Press, Oxford, pp. 111-125.
- Watson, E.B. and A. Lupulescu, 1993, Aqueous fluid connectivity and chemical transport in clinopyroxene-rich rocks, *Earth Planet. Sci. Lett.*, **117**, 279-294.
- Yamaoka, S., O. Fukunaga and S. Saito, 1970, Phase equilibrium in the system MgO-H₂O at high temperatures and very high pressures, *J. Am. Ceram. Soc.*, **53**, 179-181.
- Zhang, Y.-G. and J.D. Frantz, 2000, Enstatite-forsterite-water equilibria at elevated temperatures and pressures, *Am. Mineral.*, **85**, 918-925.

(Received July 9, 2001)

(Accepted October 5, 2001)